Electronic Supplementary Information

PdNi nanosheets with coordinated d-d orbitals for efficient ethanol electrooxidation via the C_2 pathway

Guanjun Chen[a,*], Zheming Huang[a], Yichu Lei[a], Kaiwen Yang[a], Jiayi Yang[a], Long Chen[a], Tong Wang[a], Shuhan Yang[b,*], Haibo Yang[a,*]

[a] *School of Materials Science and Engineering, Shaanxi University of Science and Technology, Xi'an, 710021, China*

[b] *State Key Laboratory for Mechanical Behavior of Materials, Xi'an Jiaotong University, Xi'an, 710049, China*

*Corresponding author:

sk-cgj@sust.edu.cn (G. J. Chen);

2746341535@stu.xjtu.edu.cn (S. H. Yang);

yanghaibo@sust.edu.cn (H. B. Yang).

Figure S1 Guanjun Chen *et al*.

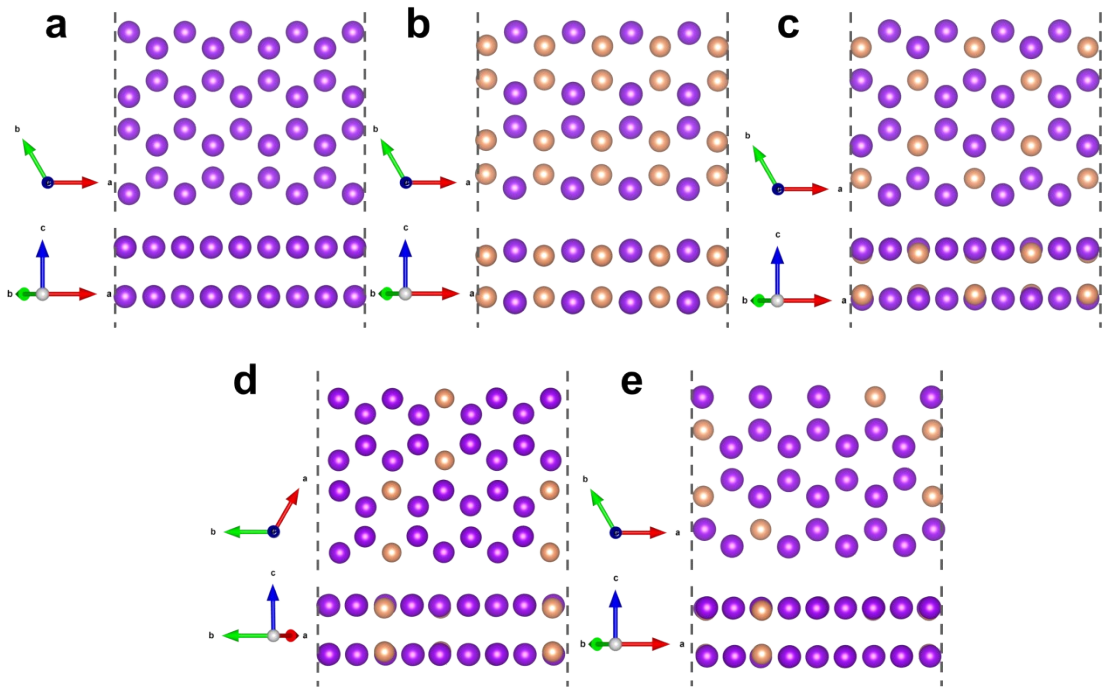

Figure S1. The optimized stable structure model of (a) Pd, (b) Pd_1Ni_1, (c) Pd_3Ni_1, (d) Pd_5Ni_1 and (e) Pd_7Ni_1.

Figure S2 Guanjun Chen *et al*.

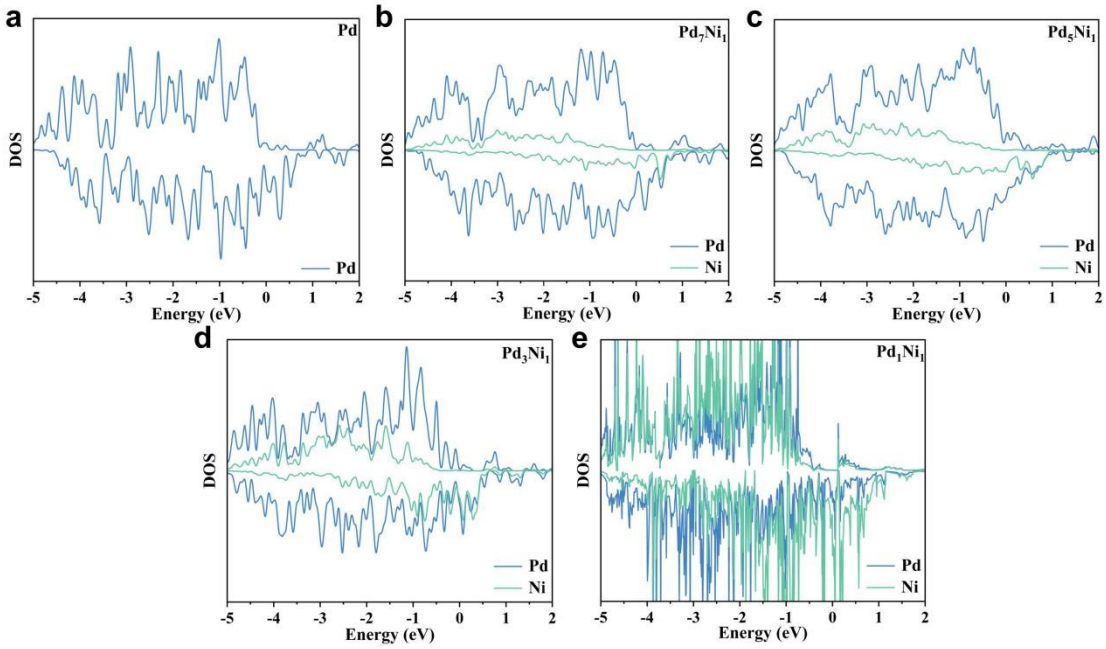

Figure S2. (a) DOS of Pd. (b-e) DOS of Pd and Ni in Pd_xNi_y.

Figure S3 Guanjun Chen *et al*.

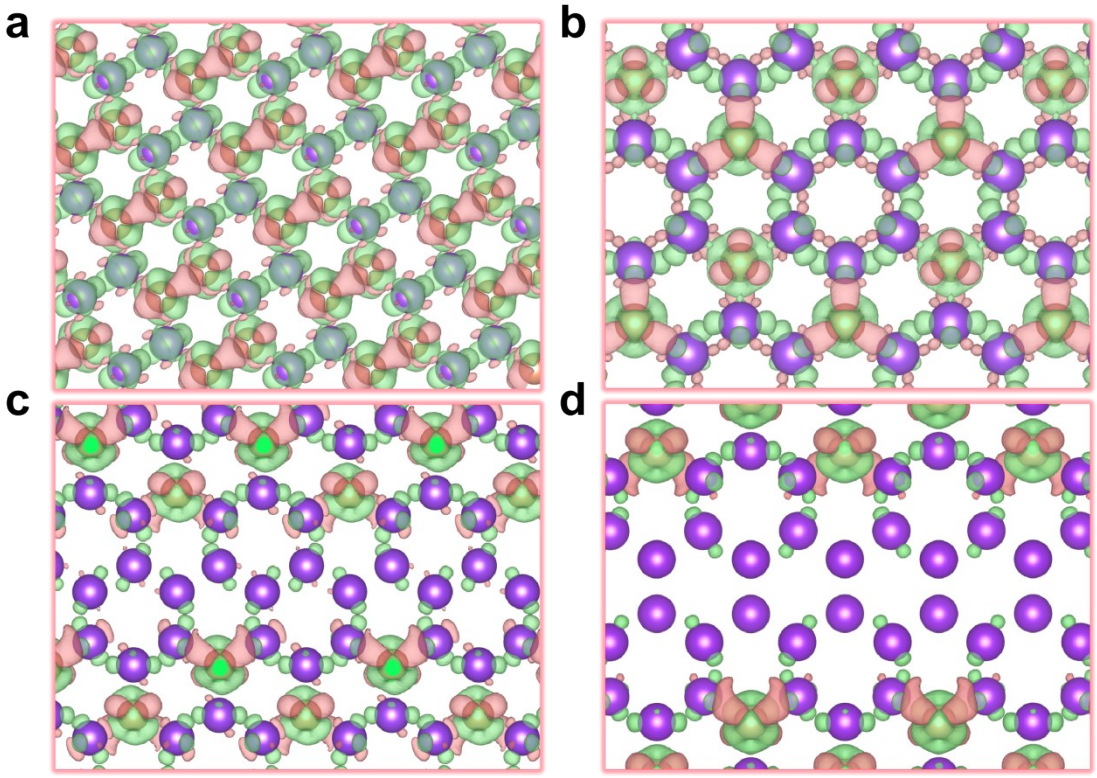

Figure S3. The differential charge distributions of (a) Pd_1Ni_1, (b) Pd_3Ni_1, (c) Pd_5Ni_1 and (d) Pd_7Ni_1. The corresponding isosurface value are set to 8×10^{-3} *e*/Å^3. Pd and Ni atoms are represented by purple and orange balls.

Figure S4 Guanjun Chen *et al*.

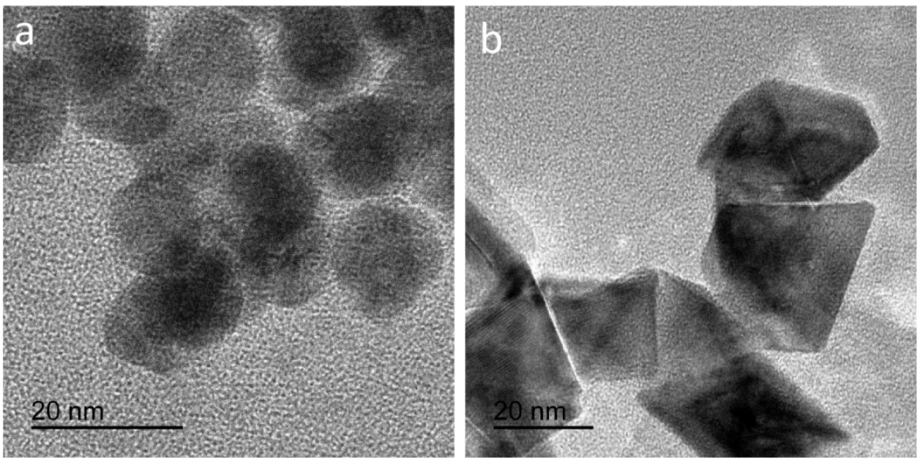

Figure S4. (a) Product obtained in the absence of $Mo(CO)_6$; (b) product obtained in the absence of CTAB.

Figure S5 Guanjun Chen *et al*.

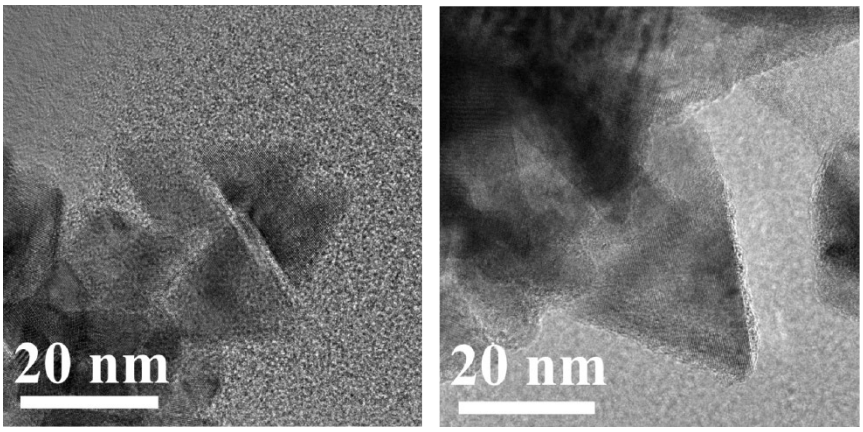

Figure S5. TEM images of Pd_xNi_y.

Figure S6 Guanjun Chen *et al*.

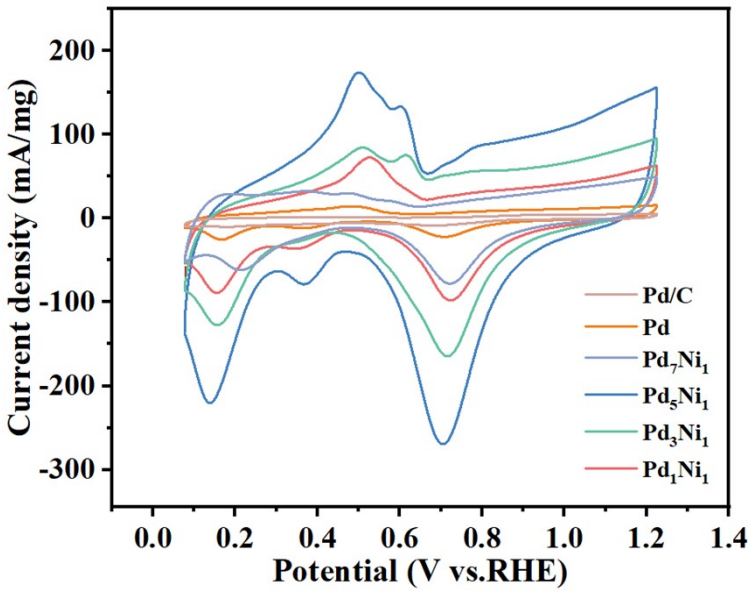

Figure S6. Stable CV curves of commercial Pd/C, Pd nanosheet and Pd_xNi_y nanosheets in 1 M KOH.

Figure S7 Guanjun Chen *et al*.

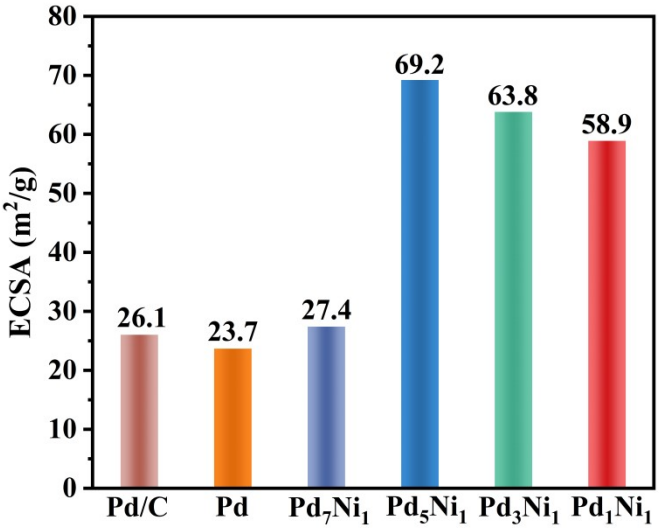

Figure S7. The ECSA values of commercial Pd/C, pure Pd nanosheet, Pd_7Ni_1, Pd_5Ni_1, Pd_3Ni_1 and Pd_1Ni_1 catalysts.

Figure S8 Guanjun Chen *et al*.

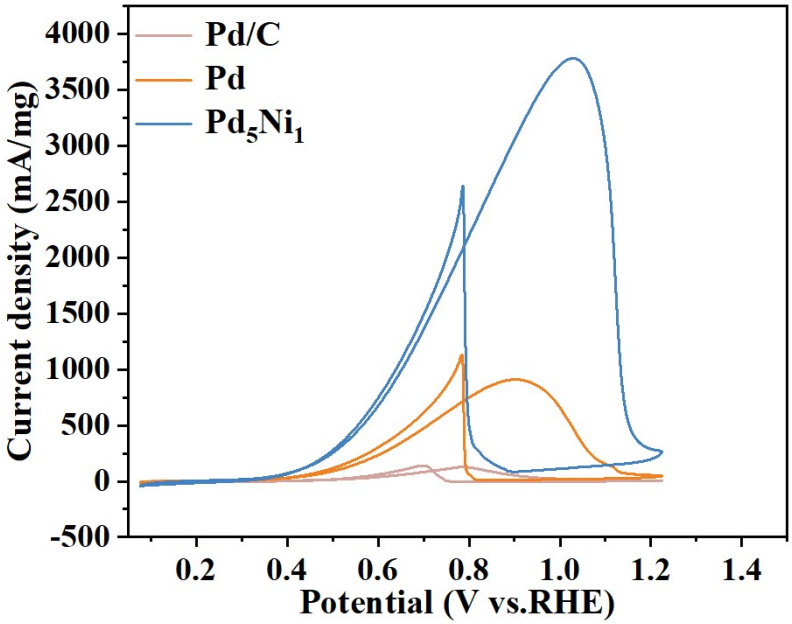

Figure S8. Stable CV curves of commercial Pd/C, Pd nanosheet and Pd_5Ni_1 nanosheet in 1 M KOH/1 M ethanol.

Figure S9 Guanjun Chen *et al*.

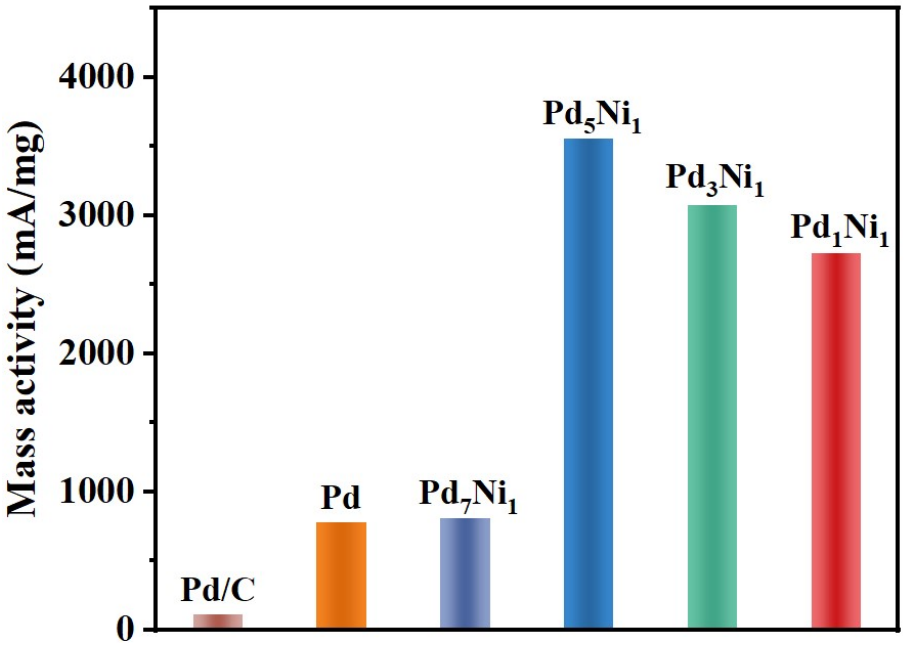

Figure S9. The maximum mass activities of commercial Pd/C, Pd nanosheet and Pd_xNi_y nanosheets.

Figure S10 Guanjun Chen *et al*.

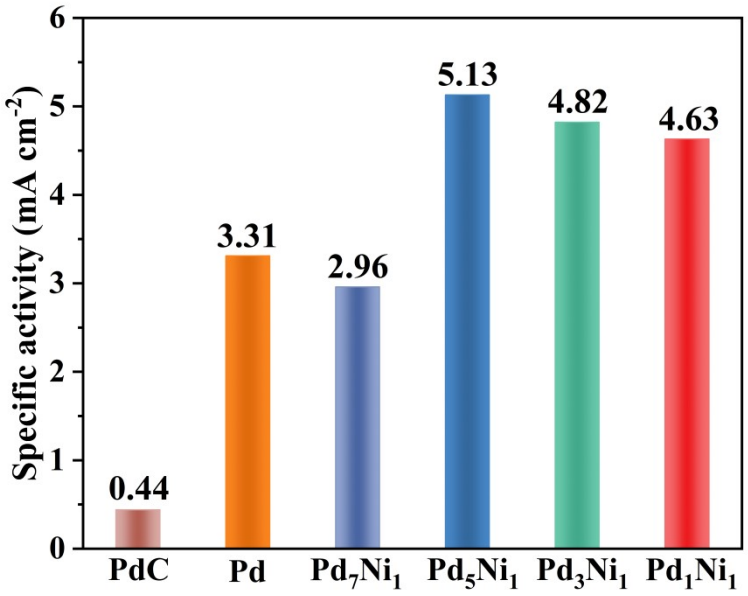

Figure S10. The specific activities of commercial Pd/C, pure Pd nanosheet, Pd_7Ni_1, Pd_5Ni_1, Pd_3Ni_1 and Pd_1Ni_1 catalysts.

Figure S11 Guanjun Chen *et al*.

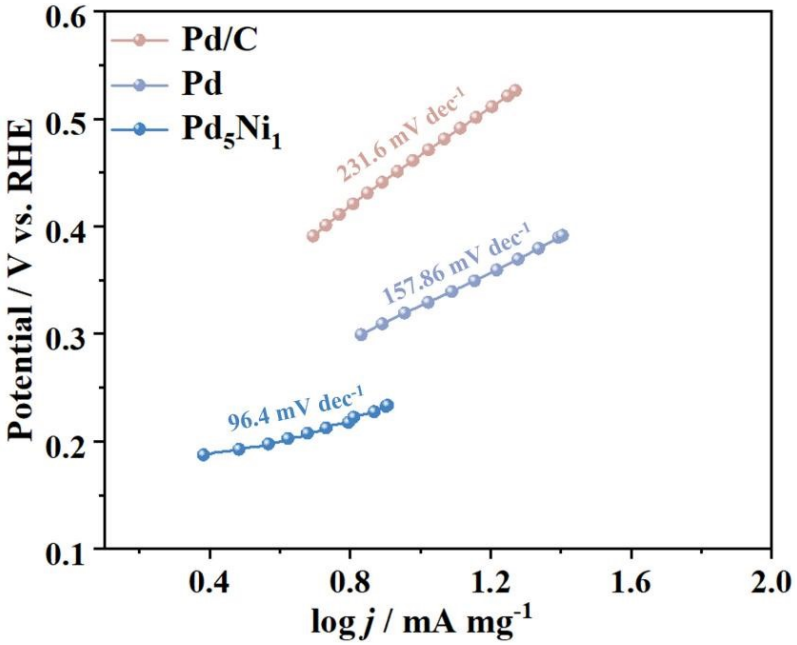

Figure S11. The Tafel slope of Pd/C, pure Pd and Pd_5Ni_1 catalysts.

Figure S12 Guanjun Chen *et al*.

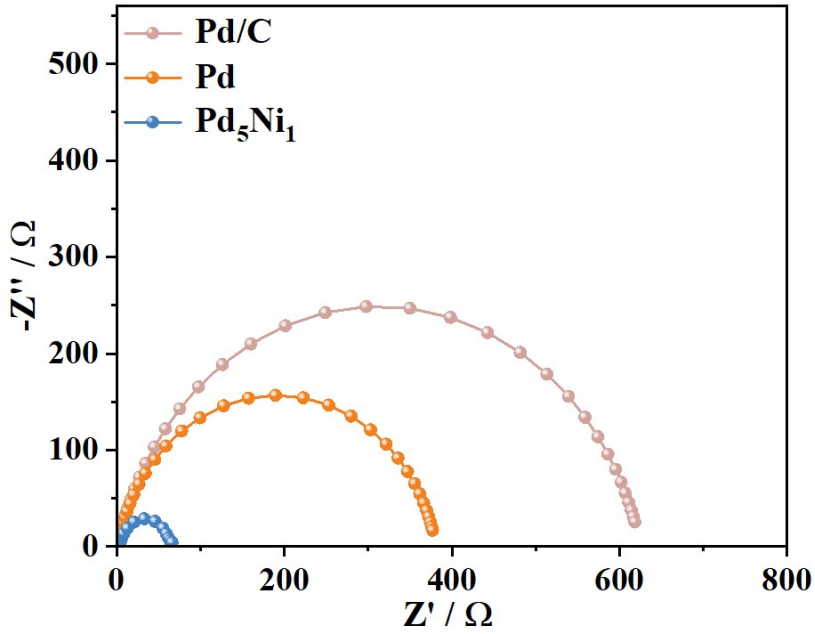

Figure S12. The EIS spectra of Pd/C, pure Pd and Pd_5Ni_1 catalysts.

Figure S13 Guanjun Chen *et al*.

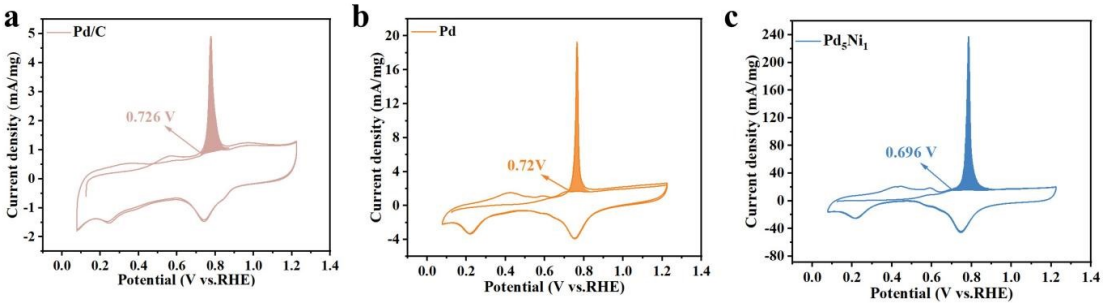

Figure S13. The CO stripping curves of Pd/C, pure Pd and Pd_5Ni_1 catalysts.

Figure S14 Guanjun Chen *et al*.

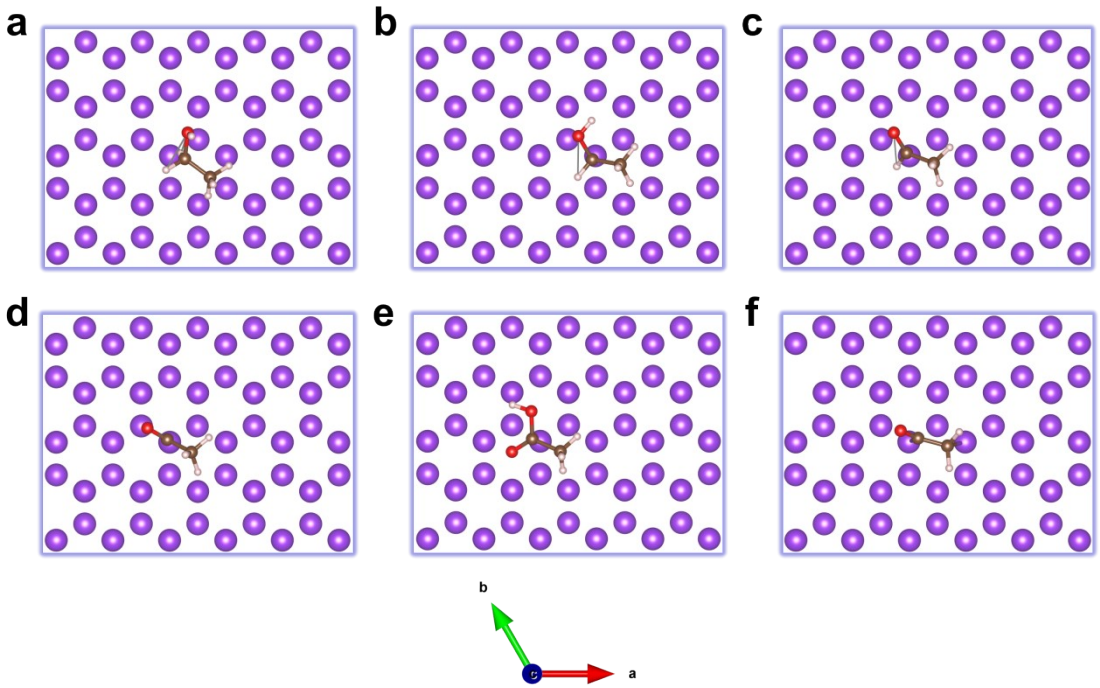

Figure S14. The stable models of (a) *CH_3CH_2OH, (b) *CH_3CHOH, (c) *CH_3CHO, (d) *CH_3CO, (e) *CH_3CHOOH and (f) *CH_2CO adsorption in Pd surface.

Figure S15 Guanjun Chen *et al*.

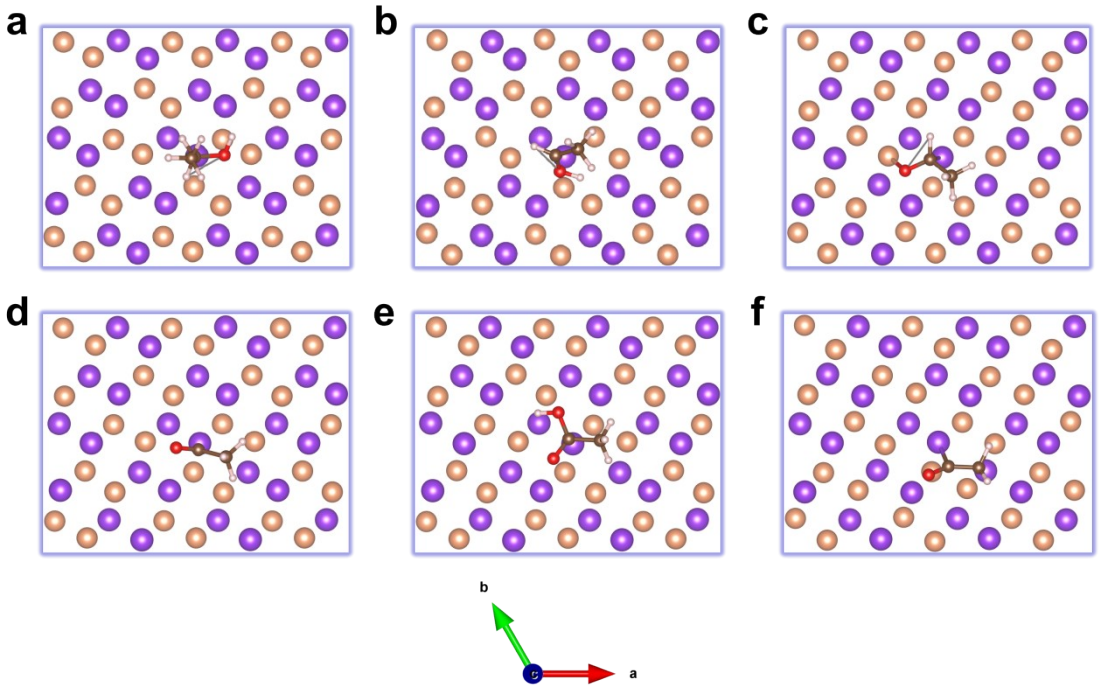

Figure S15. The stable models of (a) *CH_3CH_2OH, (b) *CH_3CHOH, (c) *CH_3CHO, (d) *CH_3CO, (e) *CH_3CHOOH and (f) *CH_2CO adsorption in Pd_1Ni_1 surface.

Figure S16 Guanjun Chen *et al*.

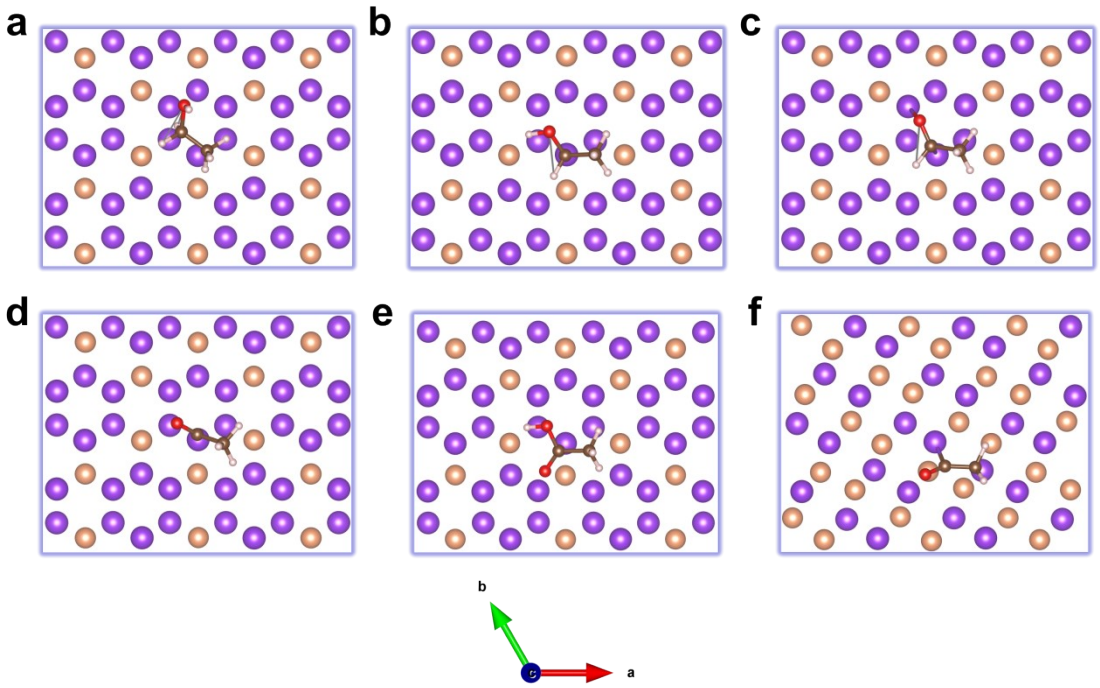

Figure S16. The stable models of (a) *CH_3CH_2OH, (b) *CH_3CHOH, (c) *CH_3CHO, (d) *CH_3CO, (e) *CH_3CHOOH and (f) *CH_2CO adsorption in Pd_3Ni_1 surface.

Figure S17 Guanjun Chen *et al*.

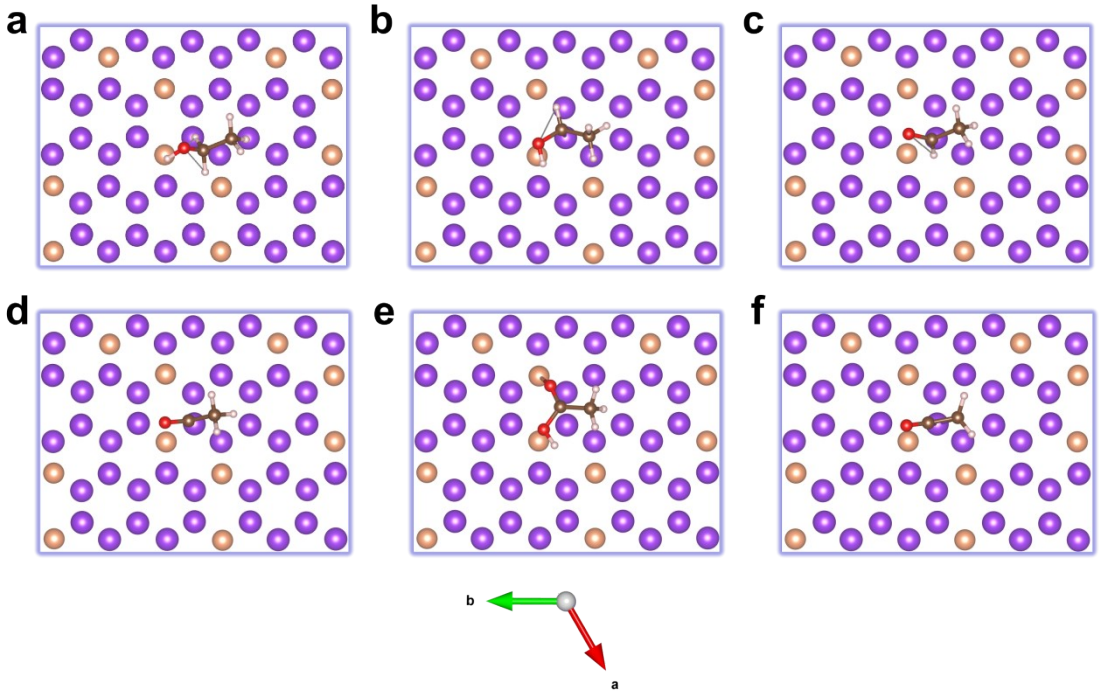

Figure S17. The stable models of (a) *CH_3CH_2OH, (b) *CH_3CHOH, (c) *CH_3CHO, (d) *CH_3CO, (e) *CH_3CHOOH and (f) *CH_2CO adsorption in Pd_5Ni_1 surface.

Figure S18 Guanjun Chen *et al*.

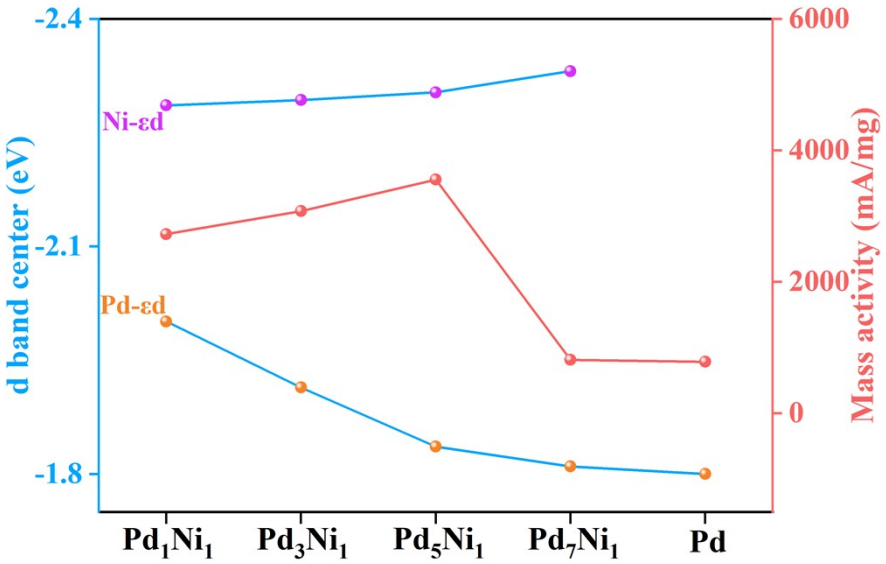

Figure S18. The the d-band centers of Pd and Ni, as well as mass activities vs. composition for the Pd_xNi_y.

Figure S19 Guanjun Chen *et al*.

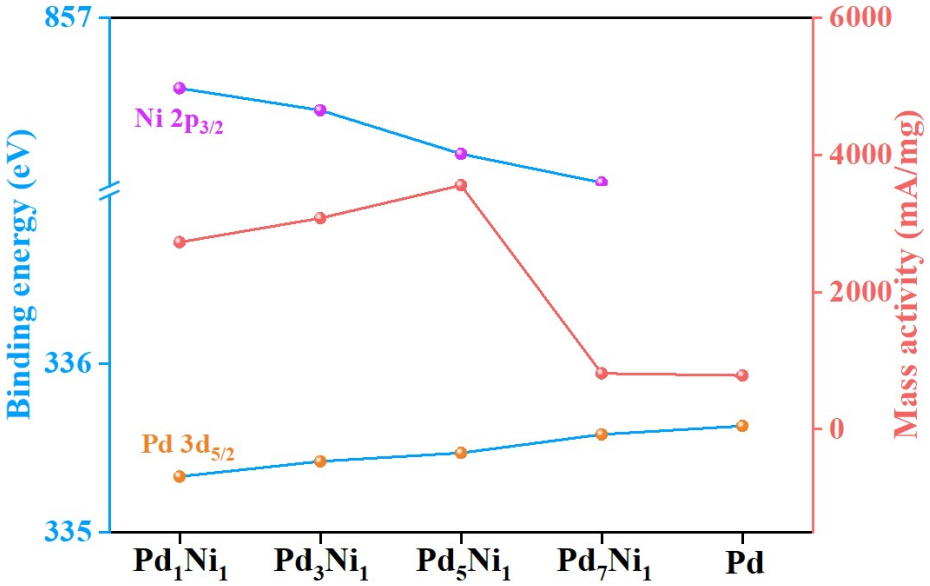

Figure S19. The binding energies and mass activities vs. composition for the Pd_xNi_y.

Table S1 Guanjun Chen *et al*.

Table S1 The calculated Pd-Pd bond length in pure Pd and Pd-Ni bond lengths in Pd_xNi_y alloy.

Sample	Pd-Pd bond length (Å)	Pd-Ni bond length (Å)
Pd_1Ni_1	--	2.589
Pd_3Ni_1	--	2.656
Pd_5Ni_1	--	2.685
Pd_7Ni_1	--	2.691
Pure Pd	2.714	--

Table S2 Guanjun Chen *et al*.

Table S2 The calculated Bader charge of surface Pd and Ni atoms for Pd_xNi_y alloy.

Sample	Bader charge (e)	
	Pd	Ni
Pd_1Ni_1	0.234	-0.235
Pd_3Ni_1	0.101	-0.297
Pd_5Ni_1	0.074	-0.335
Pd_7Ni_1	0.04	-0.340

Table S3 Guanjun Chen *et al*.

Table S3 The calculated d band center (ε_d) of surface Pd and Ni atoms for pure Pd and Pd_xNi_y alloy.

Sample	$\boldsymbol{\varepsilon_d}$ (eV)	
	Pd	Ni
Pd_1Ni_1	-2.001	-2.286
Pd_3Ni_1	-1.194	-2.293
Pd_5Ni_1	-1.836	-2.303
Pd_7Ni_1	-1.810	-2.331
Pure Pd	-1.800	--

Table S4 Guanjun Chen *et al*.

Table S4 A summary of lattice parameters of Pd nanosheets and Pd_xNi_y nanosheets.

Sample	2θ/degree (111)	Crystalline size nm	Interplanar spacing nm	Strain %
Pd_xNi_y nanosheet	40.20	8.76	0.2241	0.71
Pd nanosheets	39.85	9.38	0.2257	-

Table S5 Guanjun Chen *et al*.

Table S5 The chemical states of Pd and Ni in Pd_xNi_y alloy.

	Pd	Pd_7Ni_1	Pd_5Ni_1	Pd_3Ni_1	Pd_1Ni_1
Pd^0	72.6	70.2	74.6	72.9	73.9
Pd^{2+}	27.4	29.8	25.4	27.1	26.1
Ni^0	-	69.9	72.3	73.7	75.2
Ni^{2+}	-	30.1	27.7	26.3	24.8

Table S6 Guanjun Chen *et al*.

Table S6 The intermediate free energy of the EOR on the surface of pure Pd and Pd_xNi_y alloy.

Intermediate	Pd_1Ni_1	Pd_3Ni_1	Pd_5Ni_1	Pure Pd
$*CH_3CH_2OH$	-0.77762	-1.05768	0.38628	0.03935
$*CH_3CHOH$	-0.10713	-0.77542	0.75613	0.39442
$*CH_3CHO$	0.07458	-0.25025	1.20051	1.08950
$*CH_3CO$	0.28660	0.22291	0.90844	0.72800
$*CH_3CHOOH$	0.11194	-0.31166	0.87468	0.82667
$*CH_2CO$	1.08546	0.36258	1.87765	1.43243